

A. MILENIN\*, P. KUSTRA\*

**NUMERICAL AND EXPERIMENTAL ANALYSIS OF WIRE DRAWING FOR HARDLY DEFORMABLE BIOCOMPATIBLE MAGNESIUM ALLOYS****NUMERYCZNA I DOŚWIADCZALNA ANALIZA CIĄNIENIA DRUTU Z TRUDNO ODKSZTAŁCALNYCH BIOZGODNYCH STOPÓW MAGNEZU**

In the present paper the drawing processes of thin wire of biocompatible magnesium alloys in heated die was investigated. Due to the hexagonal close packet structure magnesium alloys have low plasticity. In order to design the technological parameters the FEM model of wire drawing process in heated die and models of yield stress and ductility were developed. The relationship between technological parameters of drawing and fracture parameters was obtained based on developed models. The maps of possible elongation for MgCa0.8 and Ax30 magnesium alloys were developed using simulations. The draft schedule for final wire diameter 0.1 mm was design assisted with FEM model in experimental part of work. Based on this draft plan the drawing process from initial diameter 1.0 mm to final diameter 0.1 mm in heated die was performed in designed by author's device.

*Keywords:* MgCa0.8, Ax30, magnesium alloys, drawing process, fracture, finite element simulation

Specjalne stopy magnezu (MgCa08, Ax30), wykazujące wysoki poziom biokompatybilności ze środowiskiem organizmu człowieka, stały się alternatywnym materiałem do zastosowania na implanty medyczne. Jednym z ich zastosowań mogą być nici chirurgiczne, służące do spajania tkanki miękkiej. Nici takie powinny mieć średnicę rzędu 0.1 mm. W związku z niską technologiczną plastycznością tych stopów zaproponowano, aby proces ciągnięcia prowadzić w podgrzewanych ciągnadłach. W pracy analizowano proces ciągnięcia w podgrzewanych ciągnadłach cienkich drutów z biokompatybilnych stopów magnezu. W celu wyznaczenia technologicznych parametrów procesu ciągnięcia użyto modelu MES, który rozbudowano o rozwiązanie cieplne w ciągnadle, funkcję naprężenia uplastyczniającego oraz model utraty spójności analizowanych stopów. W oparciu o opracowany model wyznaczono zależności pomiędzy technologicznymi parametrami procesu ciągnięcia i kryterium utraty spójności. W oparciu o symulacje numeryczne zbudowano mapy dopuszczalnych odkształceń dla stopów magnezu MgCa0.8 oraz Ax30. W części eksperymentalnej pracy w oparciu o symulacje numeryczne wyznaczono schemat odkształceń do uzyskania drutu o średnicy 0.1 mm. W oparciu o wyznaczony schemat przeprowadzono proces ciągnięcia w podgrzewanych ciągnadłach ze średnicy początkowej 1.0 mm do średnicy końcowej 0.1 mm w urządzeniu skonstruowanym przez autorów.

**1. Introduction**

Magnesium alloys are more often used in industry because of their low weight. Those alloys can be deformed in many technological processes as rolling, forging, extrusion, stamping and many other technological processes applicable at elevated temperatures [1-3]. Research [4-5] shows that additions of Ca and Li (eg. MgCa0.8 – 0.8% Ca) caused that those alloys achieve a high level of biocompatibility with the human body. Scientists from the University of Hanover developed several new biocompatible Mg-Ca alloys [6]. Thus came the idea to use those alloys on resorbable suture for stitching soft tissue [7]. That is why very thin wire with diameter about 0.1 mm is needed. Such a thin wire can be obtained in drawing process. Due to poor formability and limited ductility of Mg-Ca magnesium alloys in room temperature, drawing process of thin wire is practically impossible because of their hexagonal close packet which was shown in

works [8-9]. In the case of deformation of magnesium alloys at room temperature there are only three independent slip systems. That is why the model of ductility is very important element of FEM program for simulation of wire drawing. It enables for the optimization of the process of wire drawing on the basis of simulations. The problem of prediction of ductility for the magnesium alloys is described for upsets test [2] for wire and tube drawing process [9,10]. However, in those works only few parameters of drawing, such as the die angle and reduction ratio (elongation) are considered. Investigated in this works magnesium alloys containing aluminium and zinc (eg. AZ31, AZ80) are the well-known materials, which have a higher technological plasticity than Mg-Ca alloys. This is related to initiation of micro-cracks on grains boundaries in Mg-Ca alloys in the initial phase of the deformation which was presented in work [11]. This work is dedicated to the cold deformation of MgCa0.8 alloy. Experimental and theoretical studies in work [11] showed that the state that precedes the

\* AGH UNIVERSITY OF SCIENCE AND TECHNOLOGY DEPARTMENT OF APPLIED COMPUTER SCIENCE AND MODELLING, 30-059 KRAKÓW, 30 MICKIEWICZA AV., POLAND

appearance of microscopic cracks at the grain boundaries is the optimum state of the metal after deformation but before annealing. The appearance of these microscopic cracks in the Mg-Ca alloys is observed for the very small deformations in macro scale in comparison with the typical magnesium alloys. This explains the lower technological plasticity of Mg-Ca alloys in the multipass wire drawing. This makes the realization of the wire drawing of such alloys in the cold state in comparison with the majority of the known Mg alloys especially difficult. Therefore, it is necessary to increase the number of slip systems, for instance by raising the temperature.

In work [12] a new manufacturing technology of wire made of Mg-Ca magnesium alloys was proposed. In this technology the metal was heated by a hot die and the process of warm deformation was performed. The theoretical description of the wire drawing process with a heated die is presented in work [13]. In this work the authors have developed the mathematical model of wire drawing in the heated die. Model included solution of mechanical and temperature problem in the metal and in the die, and also the model of the yield stress and fracture of the alloys MgCa08 and ZEK100. The process of fracture was examined from the point of view of the possibility of the exhaustion ductility of material in zone of deformation. However, this is the only one possible mechanism of fracture during wire drawing in the heated die. At the output from the heated die in the wire the gradient of the temperature appears (heated metal rapidly cools). At too high temperature of die this gradient leads to the localization of deformation in the hot part of the wire and breaks after output from the heated die. Thus, there is a need of examining two possible mechanisms of fracture - exhaustion of ductility and related with this fracture in the deformation zone and also the break of wire, initiated with the gradient of temperature. Another complexity in the description of the model of material in the process of wire drawing in the heated die is related with the wide interval of the variation of the temperature of metal in this process. It was shown in the paper [14] that during wire drawing in the heated die the temperature of magnesium alloy in deformation zone changes from 20°C to temperature of hot deformation. Therefore, the material models must be valid in wide interval of temperature. The strong sensitivity of fracture to technological parameters (drawing velocity, temperature of the die, elongation per pass) was shown in those works. From the other side, the rational solution is to decrease of the interval of the variation in temperature in zone of deformation by preheating the billet directly before the entrance into the die. Technically this was realized in the developed device for the drawing process [15].

The enumerated special features of process make especially urgent the validation of the mathematical model of fracture and thermal processes by experiments. For this purpose in the work [15] was proposed the device for the wire drawing, which makes it possible to solve this task. This device provides for preheating material not only in the die, but also in the special camera before the entrance into the die. This required modifications in the FEM model of wire drawing, described in the work [13].

The purposes of this work are:

- the modification of FEM mathematical model of drawing,

related with the special features of the device for the wire drawing, which was designed by authors [15];

- the calculation of the optimum parameters of multi pass wire drawing for two alloys;
- drawing of wire in laboratory conditions from the diameter 1.0 mm to final diameter 0.1 mm on the basis of the calculated technological parameters of wire drawing;
- validation of the model of temperature and fracture;
- checking the mechanical properties and microstructure of the obtained wire.

## 2. Coupled FEM model of wire drawing in heated die

The FEM code Drawing2d was developed in work [16]. The FEM model solves a boundary problem considering such phenomena as metal deformation, heat transfer in wire, metal heating due to deformation and friction. Numerical solution of thermal problem in the die was described in work [17].

### Model of plastic deformation

Solution of boundary problem is obtained using variation principle of rigid-plastic theory:

$$J = \int_V \int_0^{\xi_i} \sigma_s(\varepsilon_i, \xi_i, t) d\xi_i dV + \int_V \sigma_0 \xi_0 dV - \int_S \sigma_\tau v_\tau dS \quad (1)$$

where:  $\xi_i$  is the effective strain rate,  $\sigma_s$  is the yield stress,  $\varepsilon_i$  is the effective strain,  $t$  is the temperature,  $V$  is the volume,  $\sigma_0$  is the mean stress,  $\xi_0$  is the volumetric strain rate;  $S$  is the contact area between the alloy and the die,  $\sigma_\tau$  is the friction stress,  $v_\tau$  is the slip velocity along area of the die.

The stress tensor  $\sigma_{ij}$  is calculated on the basis of strain rate tensor  $\xi_{ij}$ . The stationary formulation of the boundary problem is used. The strain tensor  $\varepsilon_{ij}$  is calculated by integration of strain rate tensor along the flow lines.

### FEM solution of thermal problem in metal

Thermal problem in metal was solved by applying the following method. The passage of the section through the zone of deformation was simulated. For this section at each time step the non-stationary temperature problem was examined:

$$\lambda \left( \frac{\partial^2 t}{\partial r^2} + \frac{1}{r} \frac{\partial t}{\partial r} \right) + Q_d = c\rho \frac{dt}{d\tau} \quad (2)$$

where:  $Q_d = 0.9\sigma_s \xi_i$  is the deformation power,  $c$  is the specific heat;  $\rho$  is the alloy density,  $\tau$  is the time,  $\lambda$  is the thermal conductivity coefficient (the following equations are used for Mg-Ca0.8 and Ax30 alloys:  $c = 1013.4 + 0.441t$ ,  $\rho = 1741.4 - 0.173t$ ,  $\lambda = 156.32 - 0.023t$ ). Heat exchange between the alloy and the die is defined as:

$$q_{conv} = \alpha (t - t_{die}) \quad (3)$$

where:  $t_{die}$  is the distribution of die temperature on contact area, which obtained from temperature solution in die,  $\alpha$  is the heat exchange coefficient.

The generation of heat from the friction is calculated according to the formula:

$$q_{fr} = 0.9\sigma_\tau v_\tau \quad (4)$$

### FEM solution of thermal problem in the die

The model of temperature distribution in the die is based on the solution of Fourier equation in the cylindrical coordinate system:

$$\lambda \left( \frac{\partial^2 t}{\partial r^2} + \frac{1}{r} \frac{\partial t}{\partial r} + \frac{\partial^2 t}{\partial y^2} \right) = 0 \quad (5)$$

The results of measuring temperature on the contact of die with the device for drawing were used as the boundary conditions. The thermocouples and the electronic system of the control of temperature were used for measurement.

Boundary conditions on the contact of die with the metal were assigned with the aid of the dependence:

$$q_{conv} = \alpha (t - t_{metal}) \quad (6)$$

where:  $t_{metal}$  is the distribution of metal temperature on contact area obtained from temperature solution in metal.

Thus, the problem was solved by the iterative method. The iterative process included sequential solutions of thermo-mechanical problem for the metal and the thermal problem for the die. On each iteration for the metal the temperature of the die was taken from the previous solution of thermal problem in the die. Thermal problem in the die was solved with the use of temperature in the metal obtained on the previous iteration.

In relation with the fact that developed device assumes the possibility of preheating the billet before the deformation zone, the module for calculation the temperature of billet in the zone of preheating was added into the mathematical model of wire drawing.

The model of preheating is based on the solution of the one-dimensional nonstationary equation of thermal conductivity. Initial data for this model are the temperature in the zone of heating (it is assigned according to the results of measurements) and the time of the presence of the section of billet in this zone (it depends on the length of zone and speed of wire drawing).

Ductility model and yield stress model of materials were implemented to this FE model according work [13].

### 3. Yield stress model

Yield stress model for analyzed alloys was proposed as a modified Hansel-Spittel equation [13]:

$$\sigma_s = A \exp(-m_1 t) \varepsilon_i^{m_2} \xi_i^{m_3} \left( \frac{t-20}{280} \right)^{m_6} \exp\left(\frac{m_4}{\varepsilon_i}\right) (1 + \varepsilon_i)^{m_5 t} \exp(m_7 \varepsilon_i) \xi_i^{m_8 t} t^{m_9}, \quad (7)$$

where:  $A, m_1 - m_9$  – are the empirical coefficients.

To determine the empirical coefficients of equation (7) a series of tensile tests was performed at the AGH University of Science and Technology, using a Zwick 250 upstate tester to generate the stress-strain curves of the MgCa0.8 and Ax30 alloys. The tests were performed at temperatures in range 20-300°C and strain rate in range 0.1 s<sup>-1</sup> to 1 s<sup>-1</sup>. For strain rate 10 s<sup>-1</sup> the GLEEBLE 3800 simulator was used. Experiment shows, that  $\sigma_s$  is independent on the strain rate in low temperature (below 200°C), consequently the expression  $\left(\frac{t-20}{280}\right)^{m_6}$  was added to equation (7).

The coefficients in equation (7) were determined using the inverse approach with the least squares method. The objective function was formulated as the root-mean-square difference between experimental and predicted loads. Empirical coefficient of yield stress function for MgCa0.8 and Ax30 are presented in Table 1.

### 4. Ductility and wire breaking model

The key parameter which presents ductility is called ductility function [18]. This parameter is defined by the following formula [19]:

$$\psi = \frac{\varepsilon_i}{\varepsilon_p(k, t, \xi_i)} \quad (8)$$

where:  $k$  – is the triaxiality factor,  $k = \sigma_0/\sigma_s$ .

According to the formula (8) it is possible to deform the material if the value of  $\Psi$  is less than 1. Critical deformation function  $\varepsilon_p(k, t, \xi_i)$  is obtained on the basis of experimental results for the upsetting and the tension tests. In the Drawing2d FEM code equation (8) is implemented by integration along flow line as an integral:

$$\psi = \int_0^\tau \frac{\xi_i}{\varepsilon_p(k, t, \xi_i)} d\tau \approx \sum_{m=1}^{m=m_\tau} \frac{\xi_i^{(m)}}{\varepsilon_p(k, t, \xi_i)} \Delta\tau^{(m)} \quad (9)$$

where:  $\tau$  – is the time of deformation,  $\Delta\tau^{(m)}$  – is the time increment,  $\xi_i^{(m)}$  – is the values of the strain rate in the current time,  $m$  – is the index number of time step during numerical integration along the flow line.

The numerical integration of function (9) is carried out along the flow lines. The following function of critical deformation is proposed:

$$\varepsilon_p = d_1 \exp(-d_2 k) \exp(d_3 t) \xi_i^{d_4} \quad (10)$$

Coefficients of yield stress equation (7)

TABLE 1

	A	$m_1$	$m_2$	$m_3$	$m_4$	$m_5$	$m_6$	$m_7$	$m_8$	$m_9$
MgCa0.8 [13, 14]	447.4	0.0007542	0.4485	0.2867	-0.0001899	-0.009392	2	0.8318	-0.0004359	0.007962
Ax30	146.09	0.0030879	0.28327	0.09355	-0.0103528	-0.0116167	7.61	1.2575	0.0002802	0.310637

The upset and tensile tests were done at different values of  $k, t, \xi_i$  for determine coefficients of critical deformation function (10). In next step, the FEM simulations of all experimental tests have been performed to determine changes in temperature, strain rate and  $k$  from the beginning of the test until material cracking in the experiment. Using inverse method the empirical coefficients of equation (10) were determine and are presented below:

MgCa0.8 [13]:  $d_1 = 0.03313$ ;  $d_2 = 2.130$ ;  $d_3 = 0.01167$ ;  $d_4 = -0.3130$ .  
 Ax30:  $d_1 = 0.04517$ ;  $d_2 = 1.172$ ;  $d_3 = 0.01109$ ;  $d_4 = -0.1725$ .

Equations (9)-(10) described the ductility of material in deformation zone. The second mechanism of fracture (wire breaking) is related with temperature gradient in wire after deformation zone. Process of wire breaking is related to inhomogeneity of yield stress (which corresponds to inhomogeneous temperature) along wire after deformation zone. The typical temperature distribution obtained by the infrared camera during drawing process in heated die [12] is shown on Fig. 1. Velocity of drawing was 10 mm/s, temperature of the die 350°C,  $d_0 = 1$  mm,  $d_1 = 0.92$  mm. The maximum value of temperature gradient along wire is 17°C/mm. For thin wire (0.1 mm) this gradient increased, because intensity of cooling increases with a decrease in diameter.



Fig. 1. Distribution of temperature in wire after deformation, obtained by the infrared camera

The calculation of strain localization which is initiated by gradient of the temperature along wire is possible with the aid of the FEM model without its fundamental modification. However, high accuracy with the approximation of the yield stress function and the temperature of wire is required. These conditions are satisfied in the proposed model.

Simultaneously with the strain localization with the high accuracy occurs valid the classical criterion of the breaking of wire, calculated in the place of breaking:

$$\frac{\sigma_y}{\sigma_s} < 1 \quad (11)$$

where:  $\sigma_y$  – is the drawing stress.

Strain localization in simulation with the aid of the FEM model, based on the steady-state formulation of mechanical task, will be manifested in the form a qualitative change in the form of the flow lines and strain distribution. In Drawing2d software analyses of drawing process were done using two grids – Eulerian (6 – nodes finite element) and Lagrangian grid [16]. Lagrangian grid (material flow lines) is helpful in analyzing the problem of breaking (Fig. 2,a and Fig. 2,b). Correct description of the material flow causes that the phenomenon of wire breaking is modeled automatically (Fig. 2,b and 2,c). If the temperature in process is too high, wire is overheated

after deformation zone, temperature gradient along wire increase and in consequence wire breaks outside the die (Fig. 2,c). In this experiment temperature of the die was 410°C, initial diameter of wire 1 mm, initial wire drawing velocity was 10 mm/s, analogically for simulation in Fig. 2,b.

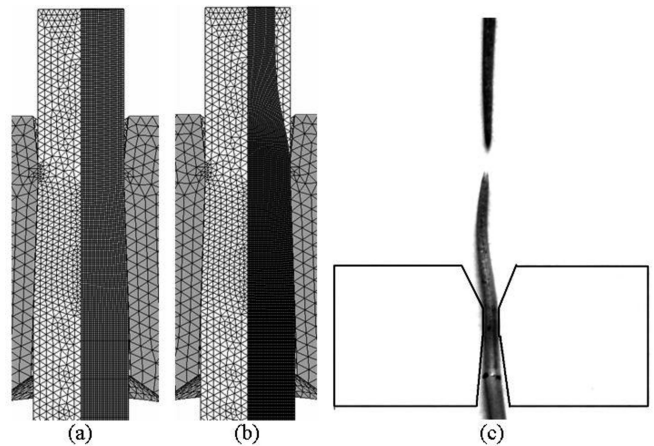


Fig. 2. Breaking of material in simulation and in experiment: (a) Eulerian (left) and Lagrangian (right) grids – material without break, (b) Euler (left) and Lagrangian (right) grids – material with break, (c) wire break in experiment

## 5. Simulation of drawing process

The first numerical simulations were performed to determine the optimal conditions for the drawing process of one pass for MgCa0.8 alloy. Several numerical simulations were done to determine the effect of the die angle, drawing velocity and elongation on distribution of effective strain and ductility function in drawing process. Common parameters for all simulations were as follows: initial diameter of wire 0.5 mm, thermal conductivity at the interface between metal and the die 10000 W/m<sup>2</sup>K, the die temperature 400°C, initial wire temperature 100°C, friction coefficient 0.1, the die angle 4°, 5°, 6°, drawing velocity in range from 0.05 m/s to 2 m/s.

Firstly, the simulations for different final diameter and die angle were considered. Simulation results are shown in Fig. 3. Distribution of ductility function and effective strain for draft  $\phi 0.5$  mm –  $\phi 0.4$  mm and different drawing angle are shown in Fig. 4 and Fig. 5.

The Fig. 3, a shows, that reducing the diameter of the final wire caused increasing of ductility function. This dependence is intuitive because in this case deformation of drawn material is higher. From the other side, increase of final diameter caused that deformation zone of the die is shorter and time of material contact with the heated tool is shorter. Therefore, temperature of material after drawing process is lower (Fig. 3,b).

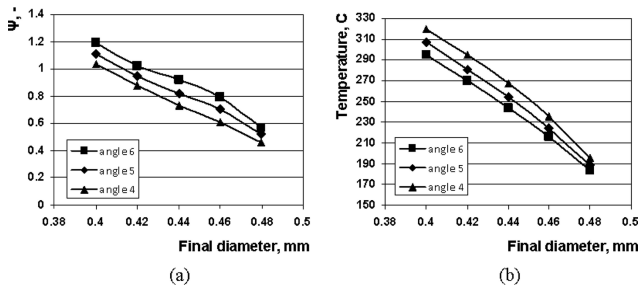


Fig. 3. Results of numerical simulation for drawing velocity 0.05 m/s and different final diameter for MgCa0.8: (a) ductility function, (b) wire temperature – in parts of wire coming out of the die

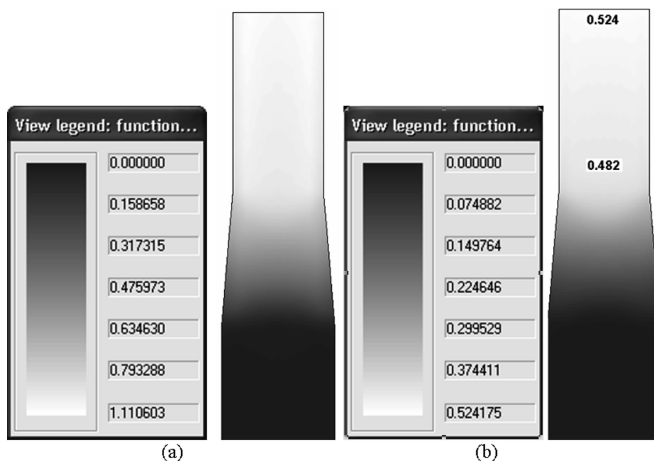


Fig. 4. Results of numerical simulation of drawing process for initial diameter 0.5 mm and final diameter 0.4 mm (elongation 1.56), drawing angle 5°, drawing velocity 0.05 m/s for MgCa0.8. Distribution of: (a) ductility function; (b) effective strain

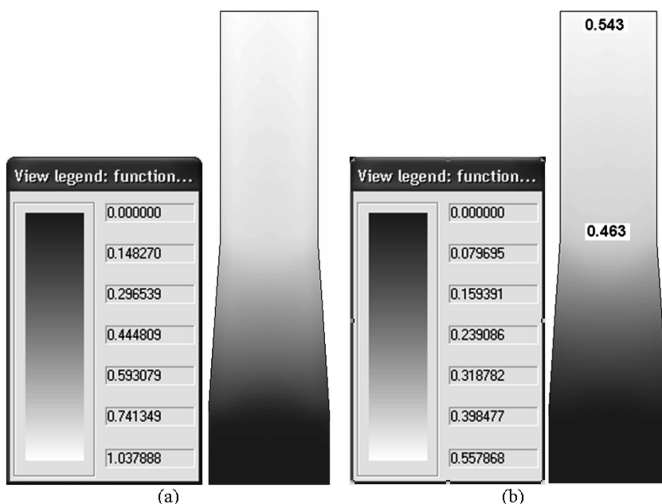


Fig. 5. Results of numerical simulation of drawing process for initial diameter 0.5 mm and final diameter 0.4 mm (elongation 1.56), drawing angle 4°, drawing velocity 0.05 m/s for MgCa0.8. Distribution of: (a) ductility function; (b) effective strain

The simulations show, that reducing of the die angle from 5° to 4° causes that the zone of highest effective strain values moves to parts of wire coming out of the die Fig. 6,b and 7,b. This state of deformation suggests that the material will break during drawing. It is effect of several facts:

1. Reduction of drawing angle results in increase length of deformation zone, so contact of drawn wire with the die is longer. The consequence of this is higher wire temperature drawn with smaller the die angle (Fig. 5,d).
2. Increasing the wire temperature causes decrease of yield stress. In analyzed example (Fig. 7,b) the drawn wire was heated by the die to temperature 319.6°C. In this case, decrease of yield stress of parts of wire coming out of the die is large enough to deform the material outside the die (wire break).

## 6. Effect of drawing speed on the material ductility

The simulations to determine influence of drawing velocity on value of ductility function were performed in the next stage of the study. Calculations for initial wire diameter 0.5 mm, final diameter 0.44 mm (elongation 1.29), drawing angle 4°, 5°, 6° and drawing velocity in range of 10 mm/s to 2000 mm/s were performed. Simulation results are shown in Fig. 6. Distribution of ductility function and effective strain for two drawing velocities 0.03 m/s and 2 m/s are shown in Fig. 9 and 10. The results presented in Fig. 7 and Fig. 9 imply that it is possible to perform of drawing process for drawing velocity in interval 10-30 mm/s.

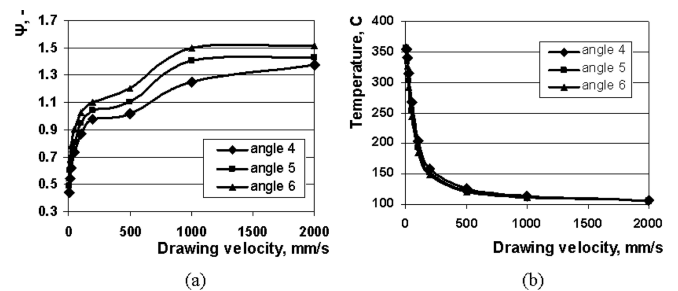


Fig. 6. Results of numerical simulation of drawing process for initial diameter 0.5 mm and final diameter 0.44 mm, drawing angle 4° ÷ 6° and different drawing velocity for MgCa0.8: (a) ductility function; (b) wire temperature after pass

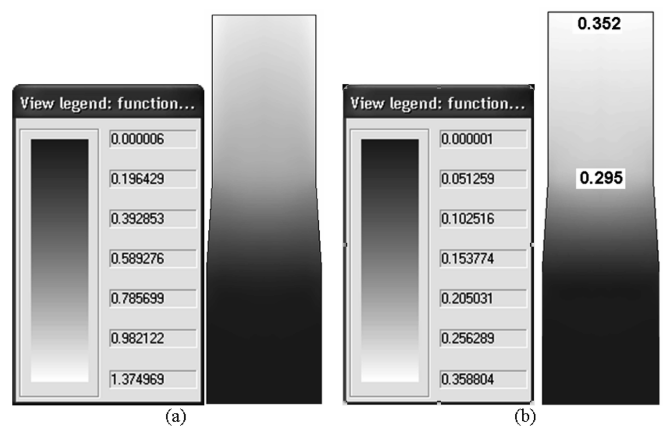


Fig. 7. Results of numerical simulation of drawing process for initial diameter 0.5 mm and final diameter 0.44 mm, drawing angle 4°, drawing velocity 2.00 m/s for MgCa0.8. Distribution of: (a) ductility function; (b) effective strain

For velocity in interval 10-30 mm/s the material is heated to a temperature about 300°C (at which recrystallization

occurs) and the ductility function reaches value less than 1.0. In addition, it should be noted that the ductility function has lower value for drawing angle 4° (Fig. 6,a). That is why this angle is applied to the multistage drawing process.

Preliminary numerical analysis shows that the drawing angle 4° is proper for this technology and this process is very sensitive to the drawing velocity. Therefore, in the next step influence of drawing velocity and value of deformation on fracture and breaking were checked. Those simulations allow developing maps of possible elongation in one pass for investigated magnesium alloys (Fig. 9-10) and temperature of the die 400°C.

Optimum temperature conditions in the Fig. 9,c and Fig. 10,c corresponds the temperature of the end of the deformation of more than 300°C. Plastometric tests, performed in the work in the work [14] showed that the dynamic recrystallization and the restoration of plasticity occur at this temperature for the majority of the conditions of wire drawing.

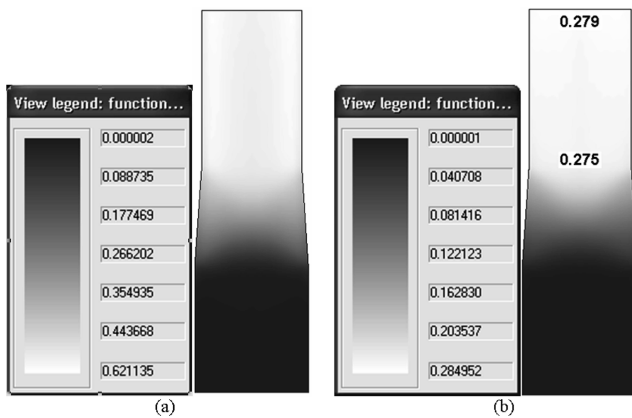


Fig. 8. Results of numerical simulation of drawing process for initial diameter 0.5 mm and final diameter 0.44 mm, drawing angle 4°, drawing velocity 0.03 m/s for MgCa0.8. Distribution of: (a) ductility function; (b) effective strain

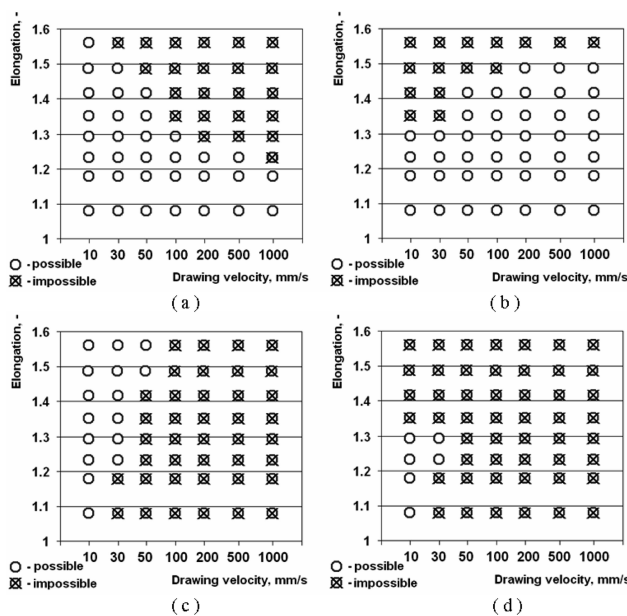


Fig. 9. Maps of possible elongations per pass for MgCa0.8 alloy: (a) according to ductility criteria (9); (b) according to wire breaking criterion (11); (c) according to optimal temperature conditions; (d) summary map

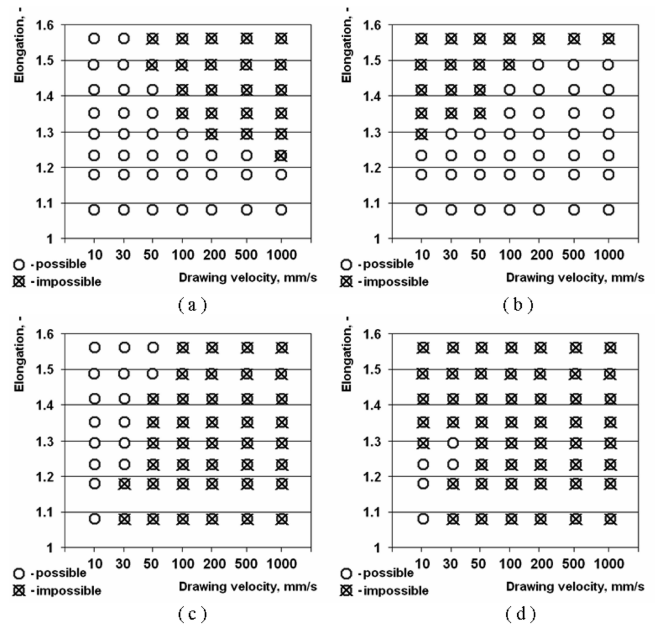


Fig. 10. Maps of possible elongations per pass for Ax30 alloy: (a) according to fracture criteria (9); (b) – according to wire breaking criterion (11); (c) according to optimal temperature conditions; (d) summary map

The value of elongation was changed to 1.21 consciously to get some safety factor due to the fact that highest value of elongation of one pass for both alloys is 1.29. Engineering calculations allowed to get draft schedule for MgCa0.8 and Ax30 (Table 2).

TABLE 2  
 Draft schedule for MgCa0.8 and Ax30 magnesium alloys

Draft	1	2	3	4	5	6	7	8	9
Diameter	0.913	0.833	0.761	0.694	0.634	0.579	0.528	0.482	0.44
Draft	10	11	12	13	14	15	16	17	18
Diameter	0.402	0.367	0.335	0.306	0.279	0.255	0.233	0.212	0.194
Draft	19	20	21	22	23	24	25	–	–
Diameter	0.177	0.162	0.147	0.135	0.123	0.112	0.1	–	–

The verification of drawing process in heated die was performed on own construction device [15] (Fig. 11) according to the scheme presented in Table 2. Drawing velocity was 10 mm/s, temperature of the die 320°C. The result of drawing process is shown in Fig. 12. Experiment shows that proposed technology is working correctly with biocompatible magnesium alloys as MgCa0.8 and Ax30.

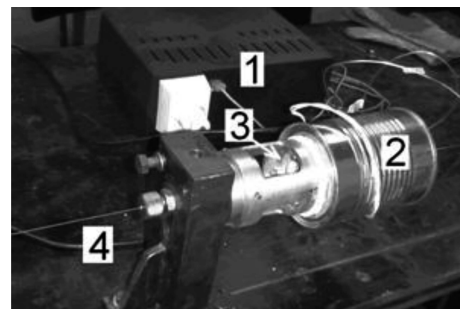


Fig. 11. Device for wire drawing in heating die – (1) electronic block, (2) heating device, (3) drawing die, (4) wire after drawing

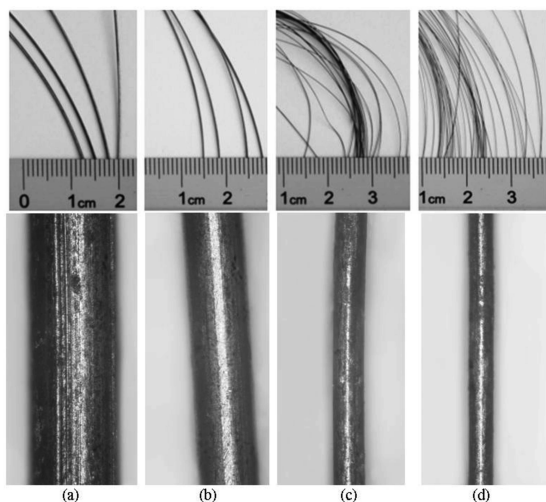


Fig. 12. Wire after drawing process of MgCa0.8 in heated die: (a)  $\phi 0.634$  mm, (b)  $\phi 0.402$  mm, (c)  $\phi 0.162$  mm, (d)  $\phi 0.100$  mm

Mechanical properties of obtained wire were tested in Instron machine before pass 1, after pass1 and after last (25) pass:

Before pass 1:  $R_m = 226$  MPa,  $A_{50} = 19,4\%$

After pass 1:  $R_m = 258$  MPa,  $A_{50} = 6,1\%$

After pass 25:  $R_m = 231$  MPa,  $A_{50} = 5,8\%$

After pass 1 plasticity of wire was decreased, it related to hardening of material and partial recrystallization. In next passes connection of preheat (in preheat chamber) and heating by the die causes full recrystallization in drawn material.

This process (recrystallization before pass, hardening and partial recrystallization during pass) was performed in stationary regime during multi-pass process. This conclusion is related to mechanical properties after last (25th) pass. The plasticity of wire in last pass was similar to plasticity after first pass.

The microstructure of Ax30 magnesium alloy wire after pass 16 is shown in Fig. 13. Partial recrystallization is observed in section along wire axis.

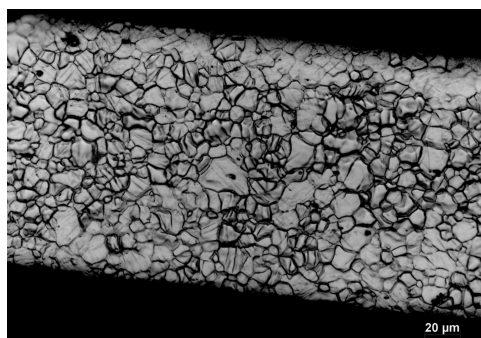


Fig. 13. Microphotographs of the microstructure of Ax30 thin wire after 16th pass

## 7. Conclusions

1. The FEM simulations and experiment have shown two different mechanisms of fracture during drawing of MgCa08 and Ax30 alloys in heated die: break of the wire at the exit section from the deformation zone and exhaustion of the ductility

of the material in the deformation zone. Break appears with the high gradient of temperature along the length of wire. This situation is observed with the high values of the temperature of die. From the other side, the exhaustion of ductility occurs at an insufficiently high temperature of metal. Thus, there is an optimum range of temperature of die, limited both on top and from below.

2. For determining the interval of the parameters of wire drawing without occurring a fracture, it is proposed the mathematical FEM model of process, which includes the modules of the calculation:

- the temperature distribution in the metal and in the die,
- the temperature of metal in the zone of preheating,
- the stress-strained state of metal,
- the yield stress and parameter of fracture.

3. Experimental studies in laboratory conditions showed that the model predict the observed mechanisms of fracture with the accuracy, sufficient for designing the technological process of wire drawing.

4. It is shown that with the use of the developed parameters of wire drawing the mechanical properties after wire drawing substantially do not change from the first to the finish pass. This makes it possible to assert that in the developed process the sufficiently complete restoration of the plasticity of material occurs.

5. The proposed technology made it possible to obtain wire 0.1 mm from the billet 1.0 mm without the application of annealing between the passages.

## Acknowledgements

The authors would like to thank the Ministry of Science and High Education of Poland, project no. 416/N-DFG-SFB/2009/0.

## REFERENCES

- [1] H. Watanebe, T. Mukai, K. Ishikawa, *J. Mater. Sci.* **39**, 1477-1480 (2004).
- [2] N. Ogawa, M. Shiomi, K. Osakada, *Int. J. Mach. Tool. Manu.* **42**, 607-614 (2002).
- [3] J. Swiostek, J. Goken, D. Letzig, K.U. Kainer, *Mater. Sci. Eng.* **424**, 223-229 (2006).
- [4] H. Haferkamp, V. Kaese, M. Niemeyer, K. Phillip, T. Phan-Tan, B. Heublein, R. Rohde, *Mat.-wiss. u. Werkstofftech* **32**, 116-120 (2001).
- [5] F.-W. Bach, R. Kucharski, D. Bormann, *Eng. Biomat.* **56-57**, 58-61 (2006).
- [6] M. Thomann, C. Krause, D. Bormann, N. Von der Höh, H. Windhagen, A. Meyer-Lindenberg, *NRW – Fundam. Clin. App.* **3**, 107-108 (2008).
- [7] J.-M. Seitz, E. Wulf, P. Freytag, D. Bormann, F.-W. Bach, *Adv. Eng. Mater.* **12**, 1099-1105 (2010).
- [8] J. Eickemeyer, A. Guth, M. Falter, R. Opitz, *Proc. 6th Int. Conf., Magnesium alloys and their Applications*, Verlg, 318-323 (2004).
- [9] K. Yoshida, *Steel Grips* **2**, 199-202 (2004).
- [10] K. Yoshida, T. Fueki, *Magnesium Technology in Global Age. MetSoc, 45 th Annual Conference of Metallurgists of CIM, Monreal, Quebec*, 587-593 (2006).
- [11] A. Milenin, D. Byrska, O. Gridin, *Computers & Structures.* **89**, 1038-1049 (2011).

- [12] A. Milenin, J.-M. Seitz, Fr.-W. Bach, D. Bormann, P. Kustra, *Wire Journal Int.*, **6**, 74-83 (2011).
- [13] A. Milenin, P. Kustra, *Steel Research Int.* **81**, 1251-1254 (2010).
- [14] A. Milenin, P. Kustra, M. Paćko, *Comput. Meth. Mater. Sci.* **10**, 69-79 (2010).
- [15] A. Milenin, P. Kustra, Sposób i urządzenie do realizacji procesu ciągnięcia cienkich drutów z niskoplastycznych stopów magnezu, zgłoszenie patentowe RP P.397292, 08.12.2011 (in Polish).
- [16] A. Milenin, *Hutnik-Wiadomości Hutnicze* **72**, 100-104 (2005).
- [17] A. Milenin, *Proc. Conf. KomPlasTech 2010*, Białka Tatrzańska, 1-9 (2010).
- [18] V. Kolmogorov, *Mechanika obrabotki metallow dawleniem*, Moscow (1986).
- [19] A. Bogatow, *Plastическая деформация сталей и сплавов*, 90-98 (1996).
- [20] A. Milenin, P. Kustra, D.J. Byrska-Wójcik, *Archives of Metallurgy and Materials* **57**, 4, 1117-1126 (2012).

*Received: 20 January 2012.*